Luminescence from β-$FeSi_2$ precipitates in Si. II: Origin and nature of the photoluminescence

L. Martinelli, E. Grilli, D. B. Migas, and Leo Miglio
INFM and Dipartimento di Scienza dei Materiali, Università degli studi di Milano-Bicocca, via Cozzi 53, 20125 Milano, Italy

F. Marabelli and C. Soci
INFM and Dipartimento di Fisica "A.Volta," Università degli Studi di Pavia, via Bassi 6, 27100 Pavia, Italy

M. Geddo
INFM and Dipartimento di Fisica, Università degli Studi di Parma, viale delle Scienze 7, 43100 Parma, Italy

M. G. Grimaldi
INFM and Dipartimento di Fisica, Università di Catania, Corso Italia 57, 95129 Catania, Italy

C. Spinella
CNR-IMM, Stradale Primosole 50, 95127 Catania, Italy
(Received 29 October 2001; published 21 August 2002)

In this paper we present photoluminescence, photoreflectance, and absorbance measurements on silicon samples with β-$FeSi_2$ precipitates, as structurally characterized in the first part of this paper [M. G. Grimaldi *et al.*, Phys. Rev. B **66**, 085319 (2002)]. By comparing the photoluminescence measurements in different experimental conditions and with excitation energy above and below the silicon threshold, by considering the direct gap estimations by photoreflectance and absorption, we argue that the 1.54 μm photoluminescence peak in the spectra is produced by an indirect transition in the disc-shaped precipitates. However, the latter ones are predicted to be the most efficient configuration, acting as a trapping well for carriers generated in the silicon matrix, and displaying a high structural quality with no dangling bonds at the β-$FeSi_2$/Si interface. Our simple model, based on band lineup at the interface, is also able to explain the temperature quenching of the photoluminescence peak.

DOI: 10.1103/PhysRevB.66.085320 PACS number(s): 78.55.Hx, 78.30.Hv, 61.72.Hh

I. INTRODUCTION

The aim of this second paper is to show that photoluminescence from the samples described in the first part of this paper[1] does originate from the particular disc-shaped precipitates (platelets) of β-$FeSi_2$ obtained at the end of range of the implanted iron. Actually we will show that it arises neither from other smaller and ball-shaped precipitates, which are also present nearby the surface, nor from defects in silicon (the well known $D1$ band[2]). In addition to that, we investigate the nature of the fundamental gap, which is still an open question.

According to absorbance, reflectance, and photoreflectance measurements, β-$FeSi_2$ single crystals and thin films (both poly and mono, prepared by different techniques) were shown to have a direct gap ranging at room temperature from 0.80 to 0.89 eV [Refs. 3–16 (Table I)]. A few papers[4,6,11] also report an indirect gap some tens of meV lower than the direct one, in agreement with most of the calculations.[17–23] However, previous photoluminescence measurements on samples with β-$FeSi_2$ precipitates[24–28] have demonstrated a signal at 1.54 μm (0.805 eV) which rapidly quenches with temperature. Moreover, it appears in literature[25–28] (and by our preliminary data, quoted in the first part of this paper[1]) that the luminescence crucially depends on the microstructure of the β-$FeSi_2$ particles and on the interface structure between them and the silicon matrix. Assessing the relationship between the direct and the indirect gaps in this material has already been attempted by several papers for epitaxial thin films.[11,29] Still defects and the microstructural changes occurring in case of precipitates need a full structural characterization of the samples (which has been outlined in Ref. 1) and a combined investigation with different optical techniques, such as photoluminescence (PL), photoreflectance (PR), and absorbance, along with a theoretical interpretation. This is what will be described in the following sections, ending up with a model which, in our opinion, is able to explain also the quenching with temperature of the PL signal, and the very puzzling question why PL arises from suitable precipitates and not from good-quality epitaxial films.

II. EXPERIMENTAL DETAILS

In order to focus our investigation on the most efficient samples analyzed in Ref. 1, here we consider two sets which have been maintained at 300 °C during the implantation of 300 keV Fe ions into float zone Si (100) (n-type resistivity of 20 Ω cm). The implantation doses of iron were 2 and 4×10^{15} at/cm^2 in order to compare the competitive action of implantation defects vs $FeSi_2$ amount. At each implantation run silicon samples both polished on one and two faces are simultaneously loaded. The beam current is kept to 0.25 μA/cm^2 to prevent unintentional beam heating. The implanted samples are suitably annealed at 800 °C for 20 h

TABLE I. Reported literature data on the value and the nature of the gap in β-$FeSi_2$. Room temperature is intended if it is not specified.

Sample type	Preparation technique	Analysis technique	Direct gap (eV)	Indirect gap $+E_{ph}$ (eV)	Ref.
Thin film	IBS and solid state react.	R&T inversion	0.80		3
Thin film 100 nm	ion implantation	Photothermal deflection	0.83	0.78	4
Polycrystalline thin film	evapotarion + RTA	Absorbance	0.84		5
Polycrystalline thin film	sputtering	Absorbance	0.84 — 0.90 (80 K)	0.83 (80 K)	6
Polycrystalline thin film	IBS on Si(001)	Transmittance	0.847 — 0.901 (10 K)		7
Thin film	EB deposition	Absorbance	0.85		8
Bulk polycristal	melting	Photothermal deflection	0.85		10
Thin film 18 and 35 nm	sublimation on Si(111)	R&T inversion	0.85		9
Epitaxial thin film	MBE deposition	Absorbance	0.87	0.765[a]	11
Thin film 670 nm	IBS on Si(001)	R&T inversion	0.87		12
Thin film	reactive deposition — SPE	Photoreflectance	0.871		13
Epitaxial thin film	MBE deposition	R&T inversion	0.89 — 0.93 (10 K)		14
Thin film	IBS on Si(100)	R&T inversion	0.89		15
Single crystal	flux transport	Photoconductivity	0.894 (80 K)		16

[a]Bare gap; the reported value for E_{ph} is 35 meV.

in a vacuum furnace at a pressure of 2×10^{-7} Torr in order to form iron disilicide precipitates and to remove the implantation damage.

One set of unimplanted samples is also thermally annealed in the same conditions to get a reference for optical investigations. In order to discriminate between the contribution of small ball-shaped precipitates formed nearby the surface and the larger platelets located at a depth between 250 and 500 nm (as described in Ref. 1), we etched both the samples prepared for photoluminescence and photoreflectance measurements (one-face polished), and for absorption measurements (two-face polished).

The etching was performed by anodic oxidation of the surface and hydrofluoric acid (HF) removal of the oxide up to 550 nm.[30] The oxidation is carried out by a galvanostat using an ethylene glycol/H_20 (3%)/KNO_3 (0.04 M) solution, and the determination of the removed silicon layers is obtained by photometric measurement of Si concentration in the HF solution. The estimation of our etching depth by the molybdenum blue method[31] turns out to be within 10% in accuracy.

We perform PL measurements exciting the samples by a 805 nm (1.54 eV) GaAs quantum well laser in the range 1×10^{-4}–5 $W\,cm^{-2}$ and by a 1300 nm (0.953 eV, below the silicon gap) InGaAs laser diode at 0.5 Wcm^{-2}, with a spot of 1 mm^2. The 805 nm laser is used to excite carriers both in β-$FeSi_2$ and Si (the penetration length is 10 μm) while the 1300 nm photons are absorbed only by the β-$FeSi_2$ precipitates. The sample temperature was varied between 13 and 200 K by a closed cycle cryocooler. Luminescence was analyzed by a 25 cm focal length single monochromator (Jarrel Ash 82/410 model), detected by a thermoelectrically cooled InGaAs photodiode with built-in preamplifier [Hamamatsu G6122S(BD2077 model)] and amplified by the lock-in technique. The reported spectra are 7 nm in resolution and 2 nm in accuracy. The reproducibility of the intensity is within 5%.

PR measurements at room temperature are performed at near-normal incidence in the 0.75–0.95 eV range, with energy steps and spectral resolution of 1 meV. A 100 W halogen lamp is used as a probe source in conjunction with a double grating monochromator. The excitation source was a 20 mW He-Ne laser and, during a second run of measurements, a 200 mW frequency doubled Nd:YAG laser, mechanically chopped at a frequency of 30 and 70 Hz, respectively. The size of the spot on the sample is about 1 mm^2 and the detector was a thermoelectrically cooled InGaAs photodiode. We find that the selected values of the modulation frequency and excitation source power optimize the signal-to-noise ratio, according to the results of Ref. 12.

We have investigated PR response of one face polished samples, in order to reduce secondary reflection from the backside. The penetration depth of both the probe source and the laser beam is high enough to reach the β-$FeSi_2$ precipitates, which lay not more than 500 nm from the surface. For this reason measurements are affected by a high offset signal because of the photoluminescence originated by precipitates and silicon. The PR background was electronically bleached by lock-in acquisition system.

Transmittance of two face polished samples implanted at different doses is measured by using two different equipment, in order to compare the results and verify any possible instrumental source of error, a double-beam, double-monochromator photospectrometer model Varian Cary 5, and a Fourier Transform Step-scan instrument model Bruker IFS66s, with a nitrogen cooled InSb detector. Low temperature measurements down to 15 K are performed with by means of a closed-circuit gas-flow cryostat. In each sample, the unimplanted substrate is taken as a reference and the absorbancies are determined with a spectral resolution of 4 nm.

Particular attention is paid to positioning the sample and to focusing the light on it, in order to obtain a high reproducibility and to avoid spurious contributions to the transmit-

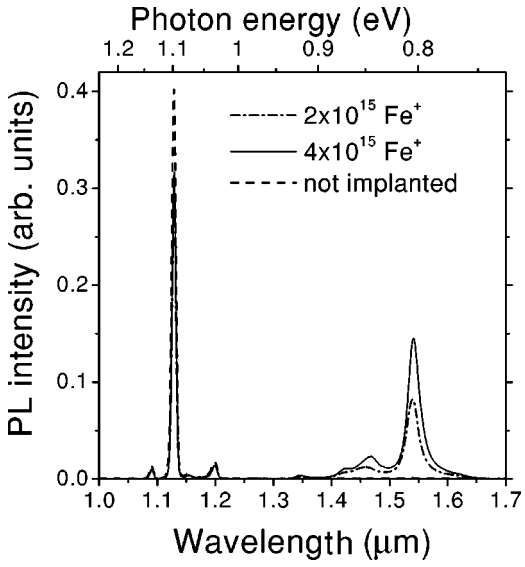

FIG. 1. PL spectra ($T=13$ K) of samples with different implantation dose of Fe. The intensity of silicon intrinsic luminescence is the same for the implanted samples.

tance; the measurements are repeated several times to control the effect of any change in the configuration. The shape of the spectra is always well reproduced, but for an error of 0.5% due to the uncertainty in the baseline, giving rise to a rigid shift of the whole spectrum (see below).

III. RESULTS

A. Photoluminescence

In Fig. 1 the PL spectra of the samples at 13 K are reported. It should be mentioned here that the intensity of the intrinsic luminescence of silicon in the region 1.09–1.20 μm (1.03–1.14 eV) is not significantly modified with respect to the one of the unimplanted sample, indicating that the crystalline quality of the implanted samples is rather good. The presented PL spectra (from 1.3 to 1.7 μm) possess four well-resolved peaks at 1.54, 1.47, 1.42, and 1.35 μm (0.805, 0.844, 0.873, and 0.918 eV, respectively) at low temperature. The most intense one is at 1.54 μm, which can be attributed to a recombination in iron disilicide precipitates and to the $D1$ band in silicon (this point will be discussed more in detail later on). The weak peaks at 1.42 and 1.35 μm are related to the $D2$ band in silicon and to a radiation damage center involving carbon, respectively.[2] The origin of the 1.47 μm peak is a donor-acceptor transition in silicon: it can be confirmed by a shift of the peak towards smaller wavelengths with increasing the pump power,[32] as is shown in Fig. 2.

As reported in a recent paper by some of us,[24] by using a low-energy Ar beam to etch the sample and by measuring the photoluminescence spectra after a progressive removal of the surface layers, it has been shown that the luminescence peak at 1.54 μm derives from the region of the sample where large platelet precipitates are located, at a depth close to the end of range of the implanted ions. However, the Ar bombardment induces structural defects in the sample, resulted in

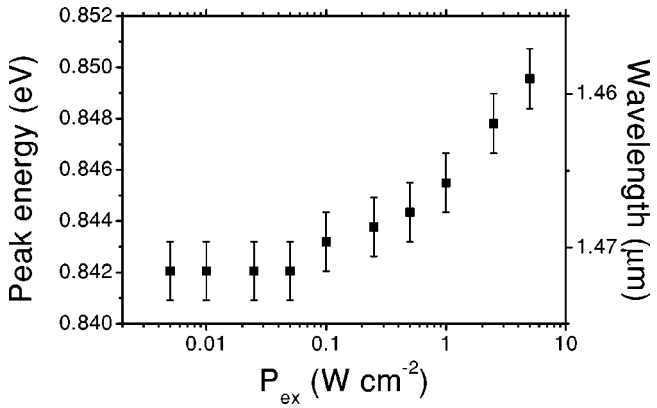

FIG. 2. Position of the luminescence peak ($T=13$ K) at about 1.47 μm as function of the excitation power for the sample implanted with 2×10^{15} at/cm^2.

a broad PL band in the 1.2–1.6 μm range (0.77–1.03 eV). In order to avoid such a damage we have repeated this experiment by using anodic oxidation and removing first 190 nm of silicon. The corresponding PL spectrum after this etching is compared to that one of the as-prepared sample in Fig. 3, demonstrating an enhancement of the 1.54 μm peak. This issue can be attributed to a greater density of free carriers reaching the platelets, because of the disappearance of the ball-shaped precipitates along with a reduction of the nonradiative recombination centers, as confirmed by the enhancement of the intrinsic silicon luminescence. After additional etching up to 380 nm (note that our sample still contains a small part of the platelets) the intensity of the peak at 1.54 μm is strongly reduced (Fig. 3), in agreement with the result obtained with the ion etching.[24] The peak finally disappears after removing up to 550 nm, the entire region where the disc-shaped precipitates are located. The residual PL signal nearby 1.54 μm can be due to dislocations ($D1$ band) in Si, as confirmed by the presence of a peak at the energy of the $D2$ band.[2]

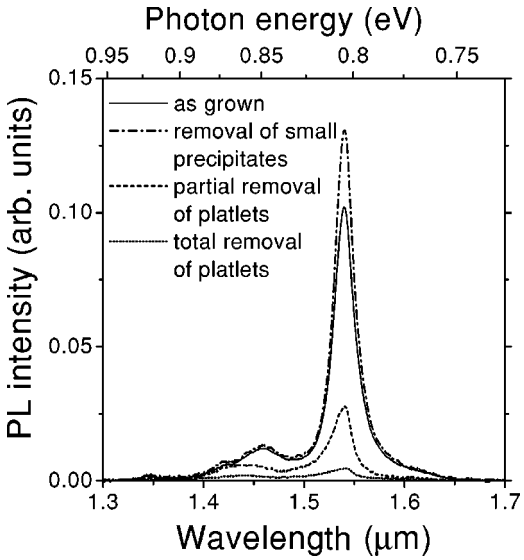

FIG. 3. PL spectra ($T=13$ K) of the sample implanted with 2×10^{15} at/cm^2 after etching (see text).

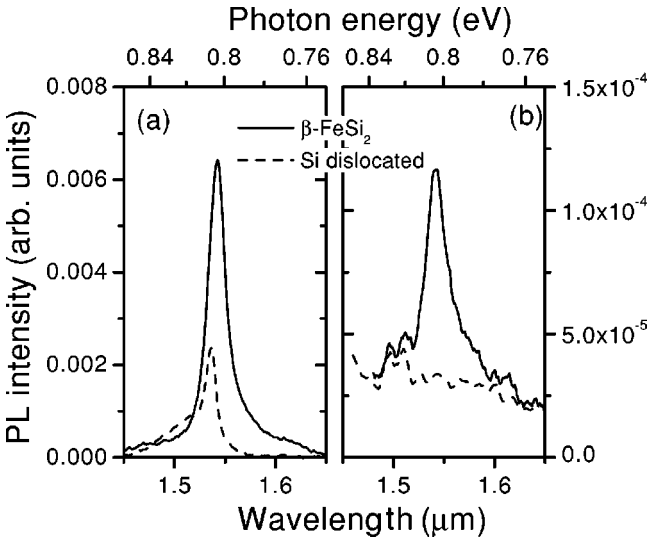

FIG. 4. PL spectra ($T=13$ K) of the sample containing β-$FeSi_2$ precipitates (solid line) and the plastically deformed silicon sample (dashed line) exciting with 805 nm (a) and 1300 nm (b) laser. In the panel b the baseline of the spectra is shifted up by the stray light of the excitation laser.

Moreover, in order to distinguish between the $D1$ band and a recombination in β-$FeSi_2$, we have measured PL spectra of a sample containing β-$FeSi_2$ precipitates and of a plastically deformed silicon sample by exciting with a 805 nm (1.54 eV) and a 1300 nm (0.954 eV) laser (Fig. 4). The photons at 805 nm should be absorbed both from Si and β-$FeSi_2$, whereas only the β-$FeSi_2$ precipitates are supposed to absorb the 1300 nm photons, as suggested by Leong *et al.*[33] By 1.54 eV excitation [Fig. 4(a)] both the samples show a similar intensity in the PL signal at about 1.54 μm: in the iron implanted sample is due to a recombination in β-$FeSi_2$ or to dislocations ($D1$ band[2]), in the plastically deformed sample is due to dislocations.

The situation is different in the case of excitation at 0.954 eV, below silicon gap [Fig. 4(b)]. These photons, lager in energy than the β-$FeSi_2$ direct gap (Table I) excite carriers into the precipitates, whereas they are possibly absorbed by dislocations through a process involving localized states at the defect core. However, a weak PL signal is visible at 1.54 μm only is the case of sample containing β-$FeSi_2$ precipitates, whereas no signal is detectable from the plastically deformed sample, indicating than the excitation below silicon gap of the $D1$ band is a very inefficient process.

This issue evidences that the 1.54 μm band is mainly due to a radiative recombination in β-$FeSi_2$ precipitates (in particular, the platelets) even if we cannot exclude the presence of some contribution also from dislocations.

We have also fitted the experimental dependence of the 1.54 μm peak position on temperature (from 13 to 215 K), by applying the semiempirical Varshni's law[32] (Fig. 5). There is no indication of any ionization of localized states in this plot and we can conclude that this emission is originated by a band to band transition in the disilicide, even at low temperature.

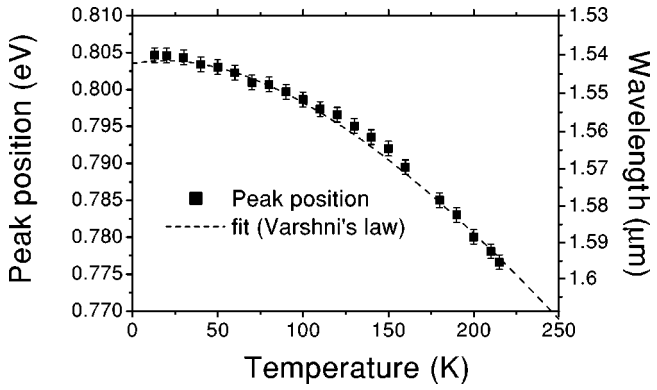

FIG. 5. Position of 1.54 μm luminescence peak as a function of temperature.

In order to distinguish the contribution of the excitation in β-$FeSi_2$ precipitates by direct photon absorption and by capture of free carriers generated in Si we have compared in Fig. 6 the PL spectra at 13 K obtained either by exciting the sample with the 805 nm laser incident from the front or from the back surface. Since the thickness of the sample (330 μm) is about 30 times larger than the penetration length of the 805 nm radiation in Si, no photons are directly absorbed by the silicide when it is excited from the back side. In this case, the PL signal at 1.54 μm is only due to carriers diffused to β-$FeSi_2$ precipitates.

It is also interesting to trace how the behavior of the 1.54 μm peak depends on the temperature and pump power. By increasing the temperature the intensity drastically lowers. The activation energy of the thermal quenching of the luminescence (Fig. 7) is estimated to be 0.23 ± 0.02 eV. Such a value is in a good agreement to the ones reported in Ref. 25 (0.2 eV) and Ref. 24 (0.26 eV). The energy of the

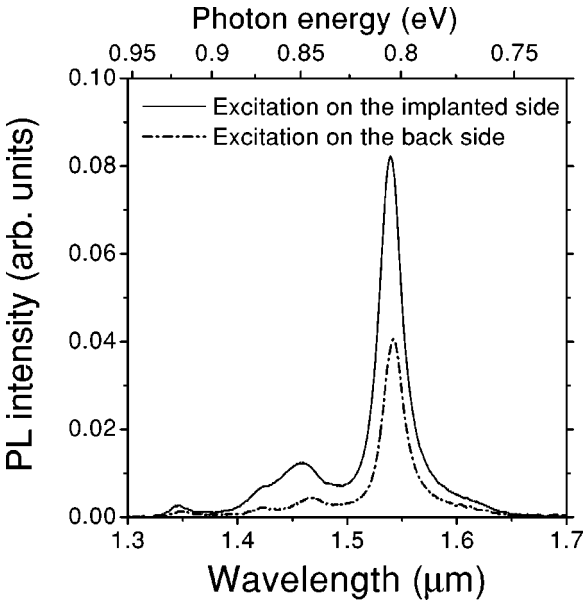

FIG. 6. PL spectra ($T=13$ K) of the sample implanted with 2×10^{15} at/cm^2 exciting on the front or back side.

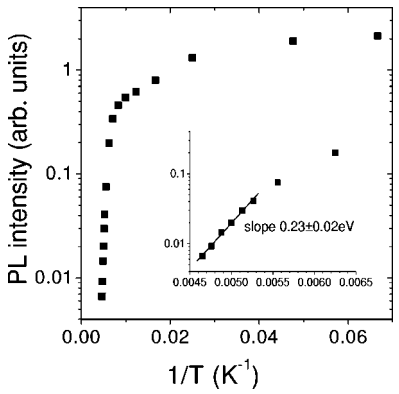

FIG. 7. PL intensity of the 1.54 μm peak as a function of temperature.

maximum and the width of the PL band at 1.54 μm are reported as a function of the pump power in Fig. 8, showing a moderate increase only for power density greater than a few W cm^{-2} as a consequence of band filling. The width of the PL peak at low excitation density at 15 K (11 meV) can be attributed to the variation in the energy gap for different platelets, because of confinement along the small width of these precipitates (some 20 nm). In order to estimate this issue, we have calculated the effective mass of electrons and holes[34,35] (summarized in Table II) in the framework of the full-potential *ab initio* method outlined in Ref. 21. An exceedingly large value for the electrons at the Λ^* point was predicted due to the very flat nature of the *d* bands. However, in the valence band maximum at the Y point, where lager *p*-state contributions are found,[11] we have $m_h = 0.25 m_e$ and the confinement energy for holes in a platelet as thick as 10 nm is about 6 meV, and it turns to 2 meV for a thickness of 20 nm. The confinement is obviously negligible in case of electrons (due to the large effective mass, Table II) and for the holes along the disc faces β-$FeSi_2$ (101) or (110).

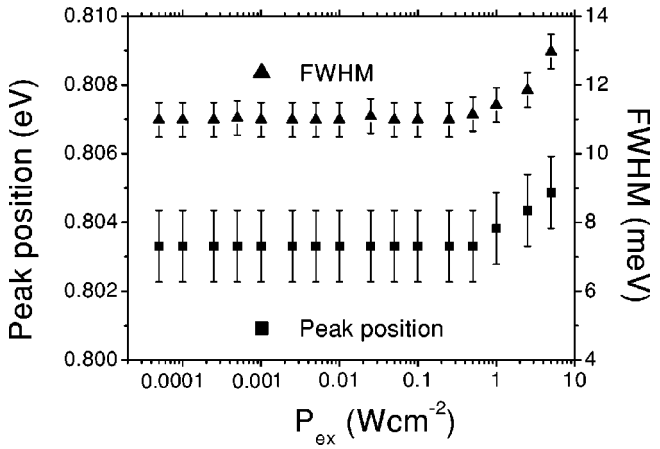

FIG. 8. Position and FWHM of the luminescence peak ($T = 13$ K) at 1.54 μm as a function of the excitation power for the sample implanted with 2×10^{15} at/cm^2.

TABLE II. The principle-axis components of the effective-mass tensor (given in units of the free-electron mass) for holes and electrons in β-$FeSi_2$.

	Λ^*			Y		
	m_{xx}	m_{yy}	m_{zz}	m_{xx}	m_{yy}	m_{zz}
Hole	1.11	0.83	0.81	0.21	0.27	0.27
Electrons		$\gg 1$		1.27	0.83	8.83

B. Photoreflectance

Photoreflectance is very useful in assessing the direct gap of the precipitates,[36] and in considering its relation to the different microstructure. In Fig. 9 the PR spectrum is reported before and after the removal of 190 nm thick surface layer. According to Aspnes[37] we have fitted the line shape of the modulated reflectance signal ($\Delta R/R$) around any critical point (CP) with the usual expression

$$\frac{\Delta R}{R} = \mathrm{Re}[Ce^{i\phi}(E - E_c + i\Gamma)^{-n}],$$

where C and ϕ are an amplitude coefficient and a phase factor, respectively. They are related to the experimental setup and to the electrooptic modulation mechanism of the native electric field at the surface of the sample. The exponent n is determined by the type of CP. Following Ref. 13, we assume a value $n = 2.5$, which is valid for three-dimensional CP describing (direct) band to band transitions in bulk samples.[37,38] E_c and Γ are the physical parameters related to the transition energy and the line broadening, respectively.

In order to fit the first of our spectra [Fig. 9(a)], taken at a modulation frequency of 30 Hz, we need a two line model which yields the values $E_{c1} = 0.81 \pm 0.005$ eV, $\Gamma_1 = 31$ meV, $E_{c2} = 0.87 \pm 0.005$ eV, and $\Gamma_2 = 17$ meV. The

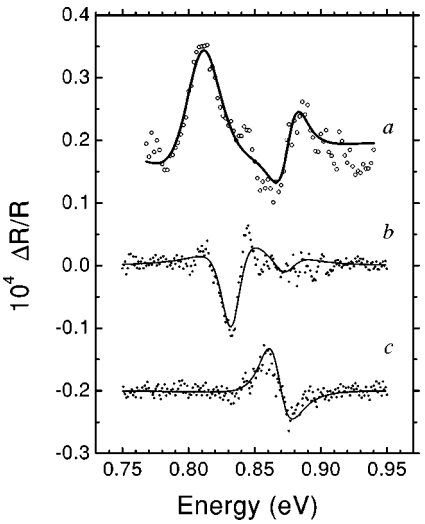

FIG. 9. Photoreflectance spectra at room temperature of samples implanted with 2×10^{15} at/cm^2: (a) using a He-Ne laser chopped at 20 Hz; (b) using a Nd:YAG laser chopped at 70 Hz before and (c) after the removing of a 190 nm layer from the sample surface.

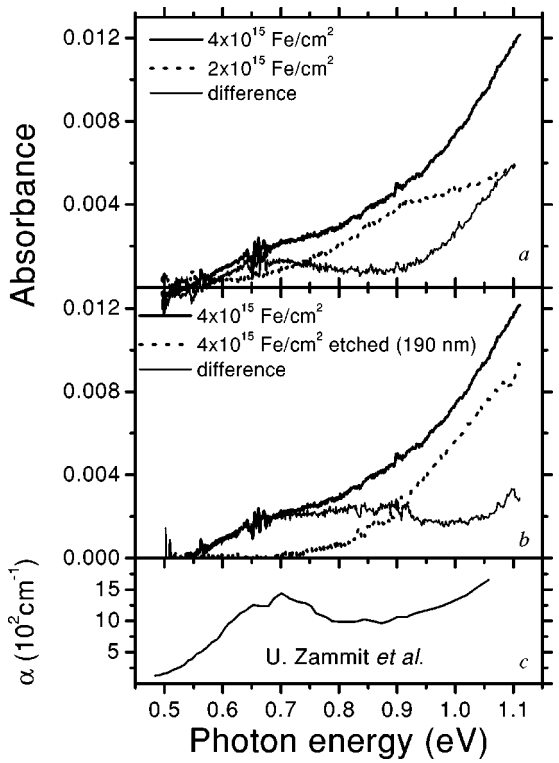

FIG. 10. Absorbance spectra ($T=300$ K) of samples with different implantation dose (a) and after etching (b), along with their difference. For sake of comparison, the absorbance spectrum of an implant-damaged sample (c) is reported from Ref. 39.

second structure corresponds to the one observed by Wang *et al.*[13] on a β-$FeSi_2$ thin film.

A further measurement on a second sample obtained with the same preparation parameters, by a more powerful laser (modulated at 70 Hz), produces the spectrum displayed in Fig. 9(b). The result is very similar to the precedent one, but for a phase change due to the different experimental conditions, and a small blueshift of the first PR feature. Finally, the measurement performed on a sample where the first 190 nm have been removed from the surface by wet etching, shows the spectrum reported in Fig. 9(c). The first structure at about 0.81–0.83 eV disappears, whereas the one at 0.87 eV increases in intensity. As a conclusion, one can ascribe the low-energy structure to small ball shaped precipitates near the surface, giving rise to a relatively big contribution to photoreflectance because of the more efficient modulation mechanism. The contribution corresponding to the large (luminescent) platelets is modulated around 0.87 eV (at room temperature), in agreement to the results obtained for thin films.[13]

C. Absorption

A complementary investigation is provided by absorbance measurements, which are, in fact, very sensitive to the defects present in the sample. Thus, it is clearly seen that the shape of the absorbance curves of the two samples with different implantation doses is not the same [Fig. 10(a)]. In this case it is also interesting to plot the difference between the two spectra [Fig. 10(a)] and compare it with the results reported in the literature concerning the implantation-related defects in silicon. The spectral features of the difference curve closely resemble those of a damaged sample by ion implantation presented in Fig. 10(c). In particular, the broad structure centered at about 0.7 eV has been ascribed to defect levels produced by implant and its strength has been correlated to the implantation doses.[39] Another defect component (such as dislocations) could also affect the absorption increase near 1 eV. Actually, some very small anomalies were observed in the low temperature absorbance spectra around 0.88 and 0.92 eV, which could be related to the detected 1.42 and 1.35 μm PL peaks. Contributions from defects should be responsible for the nonzero absorbance values between 0.5 eV and the absorption edge of iron disilicide (0.7–0.8 eV); this is particularly evident for the sample with higher implantation dose [Fig. 10(a)].

Moreover, as already observed in the PR measurements, the small ball-shaped precipitates of β-$FeSi_2$ close to the surface also affect our results. Actually, after etching about 190 nm the spectrum, which is mainly stemming from the large disk-shaped precipitates, has a sizeable increase in intensity just after 0.8 eV [Fig. 10(b)]. The difference curve here contains both defect and strained precipitate contributions, and it is slightly different with respect to the one presented in Fig. 10(a). We also note that such spurious contributions give rise to a smooth, almost constant upward shift in the absorbance at the 0.7–0.9 eV spectral region [Fig. 10(b)].

Still, as observed before, a lack of proportionality seems to exist between the absorbance intensities and the implantation dose. We found a better quantitative agreement by considering the phase and interface effects, implying a contribution to the optical response, as related to the real part of the complex refraction index and to the spatial distribution of the iron disilicide precipitates inside the substrate. By using an appropriate model of the samples (as deduced from TEM images presented in Ref. 1) and the optical functions reported in the literature[40] one can fairly well reproduce our experimental results with an iron content corresponding to the implantation doses.

Absorbance provides a characterization of the gap nature, still in our case we have to pay attention to the defect contribution. We decided (1) to take the sample implanted with the lowest dose to be the reference one, having the lowest defect density; (2) to assume that a defect-related absorbance background is affecting the results below 0.7 eV and to shift our baseline up to the value measured at 0.7 eV. The second point is essentially given ''*ad hoc*'' and can be justified on the basis of the defect spectrum shown in Fig. 10(c) and observation given in Fig. 10(b). The plot of the square absorbance vs. frequency corrected by taking the baseline is shown in Fig. 11. A similar result was obtained for the sample with the larger dose. The plot points to a direct gap value (at RT) close to the energy of the first structure observed in PR at 0.81–0.83 eV. One has to consider that the strained precipitates (as well as the defects near the surface) are also affecting the absorbance by adding a smooth contribution to it [Fig. 10(b)]. As a matter of fact, the absorbance

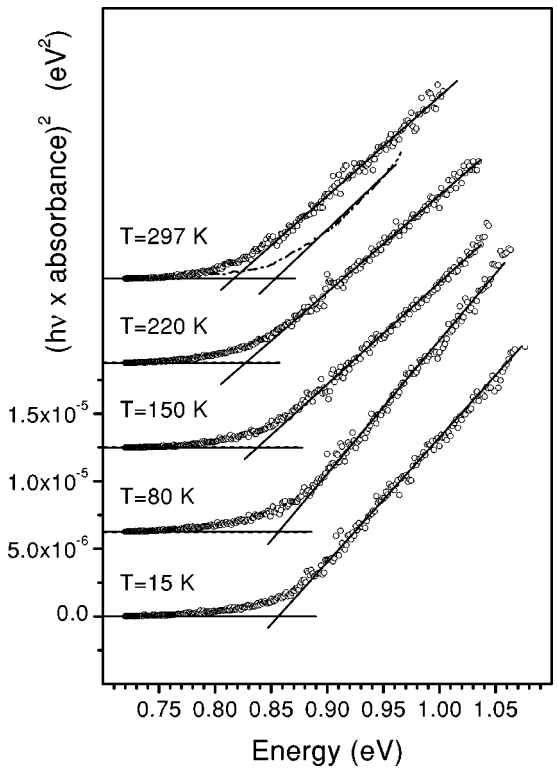

FIG. 11. Square of the absorbance spectra measured on the sample implanted with 2×10^{15} at/cm^2 at several temperatures between 15 and 300 K. The crossing of the linear behavior at the highest energies with the baseline is shown to indicate one estimation of the direct gap energy. For comparison, the room temperature spectrum of the sample implanted with 4×10^{15} at/cm^2 after the etching of the first 190 nm from the surface is also shown (dotted line). These data have been reduced by a factor 0.5 to be compared to the data of a different implant dose.

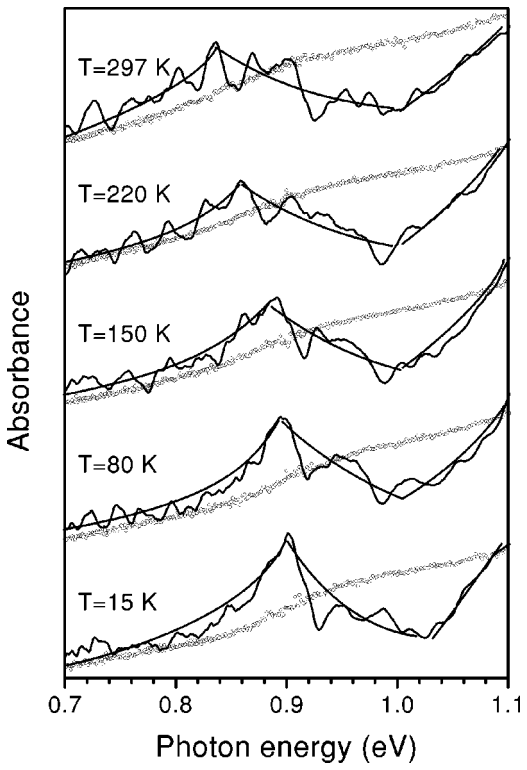

FIG. 12. Absorbance spectra measured on the sample implanted with 2×10^{15} at/cm^2 at several temperatures between 15 and 300 K. The corresponding derivatives are also shown (lines are drawn as a guide to eye).

of the etched sample at RT indicates a larger value of about 0.85 eV (Fig. 11). The most reliable evaluation of the (direct) gap of the large, disk-shaped precipitates is then obtained by finding the change in the slope of the absorbance (the peak of the first derivative[36]). Thus, in Fig. 12 the absorbancies measured on the nonetched sample are shown together with their derivatives demonstrating the evolution of the spectra with the temperature and the shift of the main structure connected with the absorption edge of β-$FeSi_2$.

The direct gap is evaluated to be 0.835 ± 0.010 eV at room temperature, increasing up to 0.900 ± 0.005 eV at low temperature. For the sake of comparison our gap values are plotted in Fig. 13 together with some results on thin films from literature.

We also tried to extend the analysis of our absorbancies to the indirect gap. Some qualitative indications of an indirect gap behavior exist, but the intensity is so low with respect to noise that any quantitative evaluation is completely hindered.

IV. MODEL AND CONCLUSIONS

Despite many data (both experimental and theoretical, several of them contradictory one with another) have been collected in literature on the origin and nature of luminescence from β-$FeSi_2$, three basic questions still remain to be assessed in the most efficient situation, which appears to be the one of the iron disilicide precipitates in silicon. Is the 1.54 μm luminescence originated by β-$FeSi_2$ precipitates or it comes from nearby defects? Is it generated by a direct or an indirect recombination of the carriers? How does the microstructure (size, morphology, and epitaxial relationship with silicon) affect the efficiency of the luminescence pro-

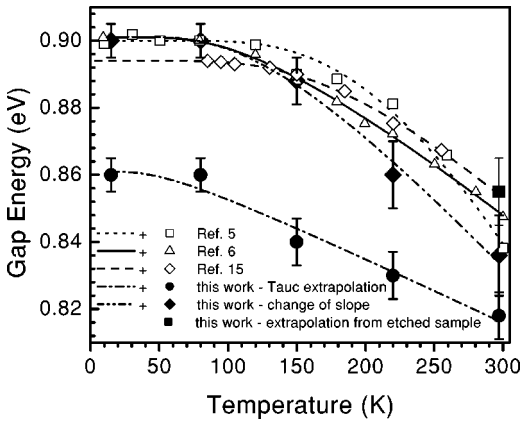

FIG. 13. Temperature dependence of direct transition (as inferred from Figs. 11 and 12) in comparison with some literature data.

cess? Here we present our interpretation and a model, which explains the activation energy of the PL thermal quenching and the rather good efficiency of the platelet configuration.

The first and the last questions are fairly well settled by many concurring experimental evidences reported in this paper: by the analysis of the TEM images and the prediction of the molecular dynamics simulation in Ref. 1, where our low-dose samples are predicted to have very few defects nearby the platelets (just behind them); by the decrease of the PL signal intensity in progressively removing the region where the platelets are located; by the PL excitation at the energy in between the gap of Si and the estimated one of β-$FeSi_2$, showing luminescence in the case of our samples, not in the case of mechanically induced dislocations in unimplanted silicon (see discussion of Fig. 4). Moreover, one additional proof will be provided by our interpretation of the activation energy for the temperature quenching in the following: to this end a good estimation of the gap size is first necessary. In fact, a wide spread of values is reported in the literature and a tentative summary of the situation is presented in Table I.

Some papers report a direct gap around 0.8 eV; some others (few ones) suggest a value larger than 0.87 eV at room temperature, whereas the most part of the references indicate a value ranging from 0.83 to 0.85 eV for the direct gap and an indirect gap 50 to 70 meV below. Actually, it is difficult to disentangle the spectral shape at the absorption edge from interference effects, impurity, and defects absorption. Moreover, the material properties themselves can also be affected by strain and orientation of the crystalline grains. The only three papers reporting the temperature evolution of the direct gap agree (despite the different sample form and measurement techniques) in finding a value around 0.9 eV at lower temperatures, decreasing down to 0.84–0.85 eV at room temperature. Such results are reported in Fig. 13 together with our data.

The position of the slope change in our absorbance spectra for precipitates (Fig. 12) almost perfectly agrees with the literature data (thin films or single crystals). The extrapolation from the plots of our results in Fig. 11 suggests a lower value for the direct gap. This is because of the contribution coming from different type of precipitates. Some of them (small and ballshaped[1]) are under stress and a variation in their gap value is expected. In particular, for the strained configuration reported in Ref. 1 we estimated by pseudopotentials calculations that the gap, still indirect, is sizeably reduced.[17] In fact, the results of photoreflectance measurements, which is a technique selectively sensitive to a direct gap related transition [band-band or exciton[41]] exhibit two structures: the one at 0.87 eV (RT) is the same as reported in the literature for this experiment on thin films; the other one, at 0.81–0.83 eV (RT), seems to be compatible with the low gap value suggested by Fig. 11. As a matter of fact our samples contain small ball-shaped nanocrystals near the surface and larger relaxed platelets at a deeper distance from the surface (as described in Ref. 1). The measurements after removing the first ones (etching 190 nm) showed the low energy structure to be related to such strained nanocrystals [Figs. 9(c) and 10(b)]. Therefore, we believe the more reliable direct gap value of the β-$FeSi_2$ platelets has to be around 0.85–0.86 eV at room temperature, as obtained on the etched sample, increasing up to 0.90 eV at the lowest temperature.

Anyway is clear that the value obtained for direct gap is incompatible with the PL structure observed at 1.54 μm (0.805 eV) at lower temperatures. From absorption measurements on our samples, becouse of the small amount of silicide present, is impossible to obtain information about the indirect gap. However, by considering the response to the 1300 nm exciting radiation and an average absorbance of 3×10^{-3} at the same wavelength, as deduced by the absorbance data, we have estimated the efficiency at 13 K of the radiative transition at 1.54 μm to be of the order of 10^{-6}, very close to the one measured for silicon intrinsic luminescence. Therefore, by assuming the 1.54 μm peak to refer to an indirect transition, also on the basis of the small PL efficiency and the long lifetime (60 μs, as reported in Ref. 24), we estimate its energy at RT by summing E_{phonon} [$\sim$0.035 eV (Ref. 11)] to the PL peack at low temperature (0.802 eV) and extrapolating the value at RT by the Varshni fit of Fig. 5. We obtain $E_g^{\mathrm{ind}}=0.776$ eV at RT, which is in good agreement with the value obtained by an absorption measurement on a epitaxial β-$FeSi_2$ film on Si,[11] when the contribution of the excitons at the absorbance is subtracted.

This picture is also consistent to the very recent full potential calculations by some of us[21] and to most of the previous *ab initio* calculations,[17–20,22,23] reporting a direct gap at the *Y* point and an indirect gap between the valence band maximum at *Y* and the conduction band minimum, approximately midway along Γ-*Z*, some 50 meV smaller. Moreover, the low value of the oscillator strength of these indirect and direct transitions has been estimated and it is shown to be an intrinsic feature of β-$FeSi_2$.[21–23] Therefore, for what concerns the second question, it is very likely that the fundamental gap nature is indirect and that it corresponds to the one estimated by PL at 0.776 eV in RT measurements.

In case of platelets an indirect transition could be efficient only if nonradiative centers are avoided and the electron-hole pairs are confined into the precipitates. In fact, the interface defects are minimized by the very good structural matching at the β-$FeSi_2$(110) or (101) interface with Si(111) on rather big area, and no dangling bonds are also predicted there.[1] Moreover, by considering the value of conduction band offset reported in Refs. 42 and 43 $\Delta E_{\mathrm{CB}}=0.22$ eV and the gap size at low temperatures of silicon (1.17 eV) and β-$FeSi_2$ (0.84 eV, as deduced from PL measurements) we obtain $\Delta E_{\mathrm{VB}}=0.11$ eV. This picture is consistent to a trapping of electron-hole pairs (mostly produced in the silicon matrix) into the disilicide (see discussion to Fig. 6), and to an activation energy of the temperature quenching (Fig. 7) equal to the energy required for the escape from the platelets of both carriers.

In conclusion we believe the poor efficiency of good quality epitaxial films to be partially related to the absence of trapping regions for the electron-hole pairs, partially to the presence of surface recombination centers. From the other

side, the low oscillator strength for interband transitions across the gap, as predicted by *ab initio* calculations[21–23] and the very limited quantity of β-$FeSi_2$ material with the suitable epitaxial relationship in the best implanted samples do restrict the application β-$FeSi_2$-diode to the case of a large injection of carriers, as it has been very recently reported by Suemasu *et al.*[44]

ACKNOWLEDGMENTS

The technical assistance of M. Moscardini for absorbance and photoreflectance measurements is gratefully acknowledged. This work was partially supported by Cofinanziamento 40% 1998 of the Italian Ministry of University and Research (Grant No. 9802154837).

[1] M. G. Grimaldi, C. Bongiorno, C. Spinella, E. Grilli, L. Martinelli, M. Gemelli, D. B. Migas, L. Miglio, and M. Fanciulli, Phys. Rev. B **66**, 085319 (2002).
[2] G. Davies, Phys. Rep. **176**, 83 (1989).
[3] V. Darakchieva, M. Baleva, M. Surtchev, and E. Goranova, Phys. Rev. B **62**, 13 057 (2000).
[4] K. Rademacher, R. Cariusm, and S. Mantl, Nucl. Instrum. Methods Phys. Res. B **84**, 163 (1994).
[5] L. Wang, L. Qin, Y. Zheng, S. Shen, X. Chen, X. Lin, C. Lin, and S. Zou, Appl. Phys. Lett. **65**, 3105 (1994).
[6] C. Giannini, S. Lagomarsino, F. Scarinci, and P. Castrucci, Phys. Rev. B **45**, 8822 (1992).
[7] Z. Yang, K.P. Homewood, M.S. Finney, M.A. Harry, and K.J. Reeson, J. Appl. Phys. **78**, 1958 (1995).
[8] S. Basu and V.L.N. Avadhani, Indian J. Phys., A **63**, 434 (1989).
[9] K. Lefki, P. Muret, N. Cherief, and R.C. Cinti, J. Appl. Phys. **69**, 352 (1991).
[10] C.A. Dimitriadis, J.H. Werner, S. Logothetidis, M. Stutzmann, J. Weber, and R. Nesper, J. Appl. Phys. **68**, 1726 (1990).
[11] A.B. Filonov, D.B. Migas, V.L. Shaposhnikov, N.N. Dorozhkin, G.V. Petrov, V.E. Borisenko, W. Henrion, and H. Lange, J. Appl. Phys. **79**, 7708 (1996).
[12] M.C. Bost and J.E. Mahan, J. Appl. Phys. **58**, 2696 (1985).
[13] L. Wang, M. Ostling, K. Yang, L. Qin, C. Lin, X. Chen, S. Zou, Y. Zheng, and Y. Qian, Phys. Rev. B **54**, R11 126 (1996).
[14] M. Rebien, W. Henrion, U. Müller, and S. Gramlich, Appl. Phys. Lett. **74**, 970 (1999).
[15] M.C. Bost and J.E. Mahan, J. Appl. Phys. **64**, 2034 (1988).
[16] E. Arushanov, E. Bucher, C. Kloc, O. Kulikova, L. Kulyuk, and A. Siminel, Phys. Rev. B **52**, 20 (1995).
[17] D.B. Migas and L. Miglio, Phys. Rev. B **62**, 11 063 (2000).
[18] L. Miglio, V. Meregalli, and O. Jepsen, Appl. Phys. Lett. **75**, 385 (1999).
[19] S.J. Clark, H.M. Al-Allak, S. Brand, and R.A. Abram, Phys. Rev. B **58**, 10 389 (1998).
[20] E.G. Moroni, W. Wolf, J. Hafner, and R. Podloucky, Phys. Rev. B **59**, 12 860 (1999).
[21] D.B. Migas, L. Miglio, W. Henrion, M. Rebien, F. Marabelli, B.A. Cook, V.L. Shaposhnikov, and V.E. Borisenko, Phys. Rev. B **64**, 075208 (2001).
[22] K. Yamaguchi and K. Mizushima, Phys. Status Solidi B **223**, 253 (2001).
[23] K. Yamaguchi and K. Mizushima, Phys. Rev. Lett. **86**, 6006 (2001).
[24] C. Spinella, S. Coffa, C. Bongiorno, S. Panitteri, and M.G. Grimaldi, Appl. Phys. Lett. **76**, 173 (2000).
[25] T. Suemasu, Y. Iikura, K. Takakura, and F. Hasegawa, J. Lumin. **87-89**, 528 (2000).
[26] T.D. Hunt, B.J. Scaly, K. Reeson, R.M. Gwilliam, K.P. Homewood, R.J. Wilson, C. Meekison, and G.R. Booker, Nucl. Instrum. Methods Phys. Res. B **74**, 60 (1993).
[27] T. Suemasu, T. Fujii, Y. Iikura, K. Takakura, and F. Hasegawa, Jpn. J. Appl. Phys. **37**, L1513 (1998).
[28] T. Suemasu, Y. Iikura, T. Fujii, K. Takakura, N. Hiroi, and F. Hasegawa, Jpn. J. Appl. Phys. **38**, L620 (1999).
[29] A. Rizzi, B.N.E. Rösen, D. Freundt, C. Dieker, H. Lüth, and D. Gerthsen, Phys. Rev. B **51**, 17 780 (1995).
[30] H.D. Barber, H.B. Lo, and J.E. Jones, J. Electrochem. Soc. **146**, 1873 (1999).
[31] F.D. Smedt, G. Stevens, S.D. Gendt, I. Cornelissen, S. Arnauts, M. Meuris, M.M. Heyns, and C. Vinckier, J. Electrochem. Soc. **123**, 1404 (1976).
[32] J. I. Pankove, *Optical Process in Semiconductor* (Prentice Hall, Englewood Cliffs, NJ, 1971).
[33] D.N. Leong, M.A. Harry, K.J. Reeson, and K.P. Homewood, Appl. Phys. Lett. **68**, 1649 (1996).
[34] In order to estimate confinement energy we used approach of effective mass approximation and also taking into account a finite depth barrier, as reported by J. H. Davies, *The Physics of Low-Dimensional Semiconductors* (Cambridge University Press, Cambridge, 1998), p. 142.
[35] The effective mass tensor for holes and electrons at the band extremum points has been evaluated by second derivatives of a five-point interpolation.
[36] M. Cardona, *Modulation Spectroscopy* (Academic Press, New York, 1969), pp. 122 and 169.
[37] D.E. Aspnes, Surf. Sci. **37**, 418 (1973).
[38] F.H. Pollak, *Handbook on Semiconductor* (North Holland, Amsterdam, 1994), p. 527.
[39] U. Zammit, K.N. Madhusoodanan, M. Marinelli, F. Scudieri, R. Pizzoferrato, F. Mercuri, E. Wendler, and W. Wesch, Phys. Rev. B **49**, 14 322 (1994).
[40] V. Bellani, G. Guizzetti, F. Marabelli, M. Patrini, S. Lagomarsino, and H. von Känel, Solid State Commun. **96**, 751 (1995).
[41] M. Cardona, *Modulation Spectroscopy* (Academic Press, New York, 1969), pp. 41–42.
[42] Okajima, H. Yamatsugu, C. Wen, M. Sudoh, and K. Yamada, Thin Solid Films **381**, 267 (2001).
[43] P. Muret, K. Lefki, T.T. Nguyen, A. Cola, and I. Ali, Semicond. Sci. Technol. **9**, 1395 (1994).
[44] T. Suemasu, Y. Negishi, K. Takakura, and F. Hasegawa, Jpn. J. Appl. Phys. **39**, L1013 (2000).